

Effects of Light and Food Schedules on Liver and Tumor Molecular Clocks in Mice

Elisabeth Filipksi, Pasquale F. Innominato, MingWei Wu, Xiao-Mei Li, Stefano Iacobelli, Li-Jian Xian, Francis Lévi

Background: Disrupted circadian coordination accelerates malignant growth, but the molecular mechanism is unclear. **Methods:** Healthy or Glasgow osteosarcoma-bearing mice (n = 162) were synchronized with light and darkness over 2–3 weeks, submitted to an 8-hour advance onset of light every 2 days (chronic jet lag) to disrupt circadian coordination, or submitted to chronic jet lag and meal timing to prevent molecular clock alteration. The expression of molecular clock genes and of the cell cycle genes c-Myc and p53 in liver and tumor was determined with quantitative reverse transcription–polymerase chain reaction at six circadian times over a 24-hour period of light and darkness and analyzed with analysis of variance and cosinor. Tumor weight was measured daily over the course of the experiment. All statistical tests were two-sided. **Results:** In synchronized mice, mean mRNA levels of clock genes *Rev-erb α* , *Per2*, and *Bmal1* varied by 206-, four-, and 26-fold, respectively, over the 24 hours in healthy mouse liver; by 36-, 35-, and 32-fold in the livers of tumor-bearing mice; and by 9.4-, 5.5-, and sixfold in tumor tissue ($P = .046$ to $<.001$). In mice subjected to chronic jet lag, the periodic changes were dampened and the clock gene rhythms were temporally shifted in liver and ablated in tumor, and tumor growth was accelerated. Meal timing reversed the chronic jet lag–induced alterations in *Rev-erb α* and *Per2* expression in liver and of all three clock genes in tumor and slowed tumor growth. Tumor growth differed as a function of light and feeding schedules ($P = .04$). No obvious rhythm was detected for p53 or c-Myc in liver or tumor tissues of synchronized mice. In healthy mice subjected to chronic jet lag, the mean level of p53 expression was cut in half ($P = .002$), and a 12-fold circadian variation in c-Myc mRNA level ($P = .03$) was induced in the liver of healthy mice, whereas complex expression patterns were found in the liver and tumor of tumor-bearing mice. **Conclusions:** Altered light–dark or feeding schedules modified the expression of molecular clock genes and genes involved in carcinogenesis and tumor progression. [J Natl Cancer Inst 2005;97:507–17]

The circadian system is responsible for the generation of approximately 24-hour rhythms in organism and cellular physiology. In mammals, the circadian system consists of circadian oscillators, which have been uncovered in the cells of most peripheral tissues and are coordinated by the suprachiasmatic nuclei, a hypothalamic pacemaker (1). The suprachiasmatic nuclei further help the organism adjust to approximately 24-hour environmental cycles. A regular alternation of 12 hours of light and 12 hours of darkness synchronizes the circadian system of laboratory rodents to precisely 24 hours, although this system normally runs with a slightly longer or shorter period in constant darkness (1–3).

The approximately 24-hour rhythms seen in most mammalian cells are controlled by a molecular clock. The molecular clock consists of interacting positive and negative feedback loops that regulate the transcription of the clock genes, 12 of which have been identified. The *Clock* and *Bmal1* genes participate in a positive feedback loop, whereas *Per* and *Cry* genes are involved in a negative feedback loop (3). A heterodimer of the *CLOCK* and *BMAL1* proteins not only rhythmically activates the transcription of clock genes *Per1*, *Per2*, *Per3*, *Cry1*, *Cry2*, and *Rev-erb α* but also activates the downstream “clock-controlled genes,” such as *D-element-binding protein (Dbp)*, *cholesterol 7 α -hydroxylase (Cyp7A)*, *glucose transporter 4 (Glut4)*, *plasminogen activator inhibitor 1 (Pai1)*, and *wee1 (1,4,5)*, which are responsible for various metabolic or proliferative functions. In turn, *Rev-erb α* negatively controls the rhythmic transcription of *Bmal1*. *PER*: *CRY* protein heterodimers further inhibit the transcriptional activity of their own genes by interfering with the activity of the *CLOCK*:*BMAL1* protein heterodimer (1,3,6).

Malignant processes result from defects in the homeostatic control of normal cellular proliferation. Environmental, surgical, and genetic conditions that disrupt the coordination of the circadian system have been shown to accelerate malignant processes in experimental models. These conditions include prolonged exposure to constant light, repeat shifts in the light–dark cycle, ablation of the suprachiasmatic nuclei in the hypothalamus, and mutations of circadian clock genes (7–12). Exposure to constant light for several weeks suppresses the rhythms in locomotor activity and body temperature, two main circadian outputs, in rats (8).

Such constant light exposure promotes liver carcinogenesis following prior initiation of malignant processes by diethylnitrosamine (8). Locomotor activity and body temperature rhythms in rodents can also be irreversibly suppressed by the physical destruction of the suprachiasmatic nuclei (2). We reported that the disrupted circadian coordination that results from suprachiasmatic nuclei lesions leads to the acceleration of the growth of a transplanted tumor (10). In healthy mice, circadian coordination can also be functionally disrupted by imposing 8-hour advances of light onset every 2 days (11). During exposure to this light–dark schedule, these mice no longer displayed

Affiliations of authors: INSERM E 0354 «Chronothérapeutique des cancers», Hôpital P. Brousse and Université Paris XI, 94807 Villejuif Cedex, France (EF, PFI, M-WW, X-ML, FL); Department of Oncology and Neurosciences, Università “G. D’Annunzio”, 66013 Chieti, Italy (PFI, SI); Cancer Center, Sun Yat-sen University, Guangzhou, China (MWW, L-JX).

Correspondence to: Francis Lévi, MD, PhD, INSERM E 0354 “Cancer chronotherapeutics” (Université Paris XI), Paul Brousse Hospital, 94800 Villejuif, France (e-mail: levi-f@vjf.inserm.fr).

See “Notes” following “References.”

DOI: 10.1093/jnci/dji083

Journal of the National Cancer Institute, Vol. 97, No. 7, © Oxford University Press 2005, all rights reserved.

a recognizable circadian pattern in rest–activity cycles or body temperature. Moreover, the growth rate of a tumor transplanted into mice submitted to such chronic jet lag was accelerated compared with that in synchronized mice (11).

The complex machinery of the molecular clock has recently been shown (5,12,13) to exert a negative effect on the transcriptional activity of some key genes involved in cell cycle regulation, thereby suggesting that the circadian clock regulates cell proliferation. Indeed, circadian rhythms in cell cycle phase distribution have been extensively reported in both healthy and malignant mammalian tissues (14–17). Two recent studies have further identified the cell cycle genes *c-Myc*, *p53*, and *Wee1* as clock-controlled genes (5,12). These genes have multiple cell cycle–related functions, with *c-Myc* and *Wee1* controlling cell cycle progression from G_1 to S and from G_2 to M , respectively. In addition, *c-Myc* can exert proapoptotic effects through *p53*-dependent or -independent pathways (18–20). Many other cell cycle–related genes display 24-hour rhythms in mRNA and/or protein expression in healthy tissues from rodents and/or humans. These genes include *cdk2*; cyclins A, B1, D, E, or *mdm2*, which control cell cycle checkpoints; or *gadd45 α* , *bcl2*, and *bax*, which regulate apoptosis (5,12,15,21,22).

The molecular circadian clock exerts a rhythmic negative regulation on cell cycle progression, which possibly accounts for a tumor suppressor–like effect of the circadian clock in the context of γ radiation exposure (12). Indeed, mice with a constitutive mutation of clock gene *Per2* not only lose circadian rhythmicity in locomotor activity when kept in constant darkness but are more susceptible to develop γ -radiation–induced cancers than wild-type mice (12).

Similarly, chronic jet lag, a condition that accelerates growth of transplanted tumors, also ablates the rhythms in mRNA expression of clock genes *Per2* and *Rev-erba* both in the liver and in the tumor of mice with Glasgow osteosarcoma (11). By contrast, meal timing, a condition that resets circadian clocks in peripheral tissues (23,24), slows down tumor growth in mice (25).

Taken together, the results of the studies mentioned above support the finding that the circadian system exerts a negative regulation on malignant processes, be it through circadian physiology and/or molecular clocks (1,22). Here, we investigated whether the disrupting effect of chronic jet lag on the molecular circadian clock would, in turn, affect the mRNA expression of *c-Myc* and *p53* and ultimately increase tumor cell proliferation. Two experiments were carried out to assess the effects of chronic jet lag on the 24-hour patterns in the expression of these clock genes and clock-controlled genes in the liver of healthy mice (experiment 1) or tumor-bearing ones (experiment 2). In experiment 2, we further investigated whether meal timing could prevent jet lag effects upon the molecular clock and downstream clock-controlled genes both in liver and in tumor of mice with Glasgow osteosarcoma. Clock genes are expressed in this tumor whose growth rate and chemosensitivity are controlled by the circadian timing system (10,11,26). Although it is known that meal timing can entrain the rhythmic expression of clock genes and clock-controlled genes in liver, no such effect has been documented in tumor.

METHODS

Animals and Synchronization

The study was conducted in accordance with the guidelines approved for animal experimental procedures by the French

Ethical Committee (decree 87-848). B6D2F₁ male mice ($n = 162$), 6–8 weeks old (Charles Rivers, L'Arbresle, France) were kept in an autonomous chronobiologic facility at a constant temperature (mean $^{\circ}\text{C} \pm$ standard deviation [SD] = 23 ± 1) that comprised six compartments, each provided with filtered air (mean flow rate, L/min \pm SD = 100 ± 10) and separate lighting regimens (Jouan, Saint-Herblain, France). Each compartment was lit with a fluorescent tube, starter TF 13 BI (Mazda Philips, Chalon-sur-Saône, France), with a light spectrum of 4100 $^{\circ}\text{K}$ and a light efficiency of 58–80 lumens/W. This light intensity corresponds to normal sunlight near midday on a mildly cloudy day. The mean light intensity (lux \pm SD = 318 ± 99) in the middle of each compartment (range = 240–580) and 129 ± 38 at each side (range = 100–220). Mice had a radio transmitter (Physio Tel, TA 10 TA-F20; Data Sciences, St. Paul, MN) implanted into their peritoneal cavity that recorded locomotor activity and body temperature every 10 minutes throughout the experiment (10).

The mice were synchronized to standard lighting conditions of 12 hours of light followed by 12 hours of darkness for 2–3 weeks and then were randomly assigned either to remain in this lighting regimen (group A) or to undergo experimental chronic jet lag produced by 10 days of serial 8-hour advances of light–dark cycle every 2 days (group B). In experiment 2 only, a third group of mice (group C) underwent chronic jet lag and concurrent meal timing from circadian time (CT) 12, ie, subjective time of onset of darkness (activity) to CT 24, i.e., subjective time of onset of light (rest). Meal timing was shown to entrain circadian expression of clock genes in the liver of mice with ablated suprachiasmatic nuclei (27), a condition that also disrupts circadian rhythms of activity and temperature (27). There were 60 control and 60 jet-lagged mice in experiment 1 and 13 control, 14 jet-lagged mice, and 15 mice that underwent jet lag and meal timing in experiment 2. Mice were weighed three times a week throughout each experiment. Experiments 1 and 2 lasted 5 and 6 weeks, respectively.

Tumor Implantation

Mice were anesthetized with a single intraperitoneal injection of 0.5-mL solution of 10 g of 2,2,2-tribromoethanol (Fluka, Saint-Quentin-Fallavier, France) in 10 mL of 2-methyl-2-butanol (Fluka) diluted 1 : 39 in 0.9% NaCl. Ten days after the beginning of chronic jet lag, eventually combined with meal timing, all the mice in experiment 2 received a subcutaneous implantation of a 3-mm³ fragment of Glasgow osteosarcoma in both flanks (10). The growth of this transplanted tumor has previously been shown to be regulated by the hypothalamic clock (10). Tumor weight was measured daily, as previously described (10).

Tissue Sampling

Ten days after the beginning of chronic jet lag (experiment 1) or 15 days after tumor inoculation (experiment 2), subgroups of mice from each group were killed at one of six different circadian times separated by 4 hours. The sampling circadian times were relative to the time of light onset, CT0. All mice were exposed to constant darkness during the 2 days preceding sampling to prevent any masking effect of light on circadian rhythms (28). There were 10 control and 10 jet-lagged mice per time point in experiment 1 and two or three mice per time point and per group in experiment 2. Approximately 30 mg of liver (experiment 1) or

liver and tumor (experiment 2) was surgically removed from each mouse, frozen immediately in liquid nitrogen, and stored later at -80°C until RNA extraction.

Quantitative Reverse Transcription–Polymerase Chain Reaction

Circadian expression patterns were determined for the clock genes *Per2*, *Cry1*, *Bmal1*, and *Rev-erba* and the cell cycle–controlled genes *c-Myc* and *p53* in the liver of healthy mice in experiment 1. In experiment 2, circadian expression was measured for *Per2*, *Bmal1*, *Reverba*, *c-Myc*, and *p53* in liver and in tumor samples.

Total RNA was extracted from the frozen tissue specimens using GenElute Mammalian total RNA kit (Sigma-Aldrich Chimie, St. Quentin-Fallavier, France) for experiment 1 or RNeasy Mini Kit (Qiagen S.A., Courtaboeuf, France) for experiment 2, according to the manufacturers' instructions. Extracted RNA concentration and purity were assessed by optical density at 260 and 280 nm. RNA integrity was assessed by the visualization of 18S and 28S RNA subunits following 1 *M* formaldehyde–1% agarose gel electrophoresis and ethidium bromide staining (0.01 $\mu\text{g}/\text{mL}$) (29). The RNA was stored at -80°C until use.

All oligonucleotide primers for PCR were obtained from Invitrogen Life Technologies (Cergy Pontoise, France). All primer pairs were designed with at least one primer comprising two successive intron–exon splicing sequences of the appropriate gene to avoid amplification of contaminating genomic DNA. Respective forward and reverse sequences of primers were as follows: 5'-ATG TGC AGC TGA TAA AGA CTG G-3' and 5'-AGG CCT TGA CCT TTT CAG TAA G-3' (ARP/36B4); 5'-GTG AAG CAG GTG AAG GCT AAT G-3' and 5'-AAG CTT GTA AGG GGT GGT GTA G-3' (*Per2*); 5'-TGG CCT CAG GCT TCC ACT ATG-3' and 5'-CCG TTG CTT CTC TCT CTT GGG-3' (*Rev-erb- α*); 5'-TGT CAC AGG CAA GTT TTA CAG AC-3' and 5'-ACA GTG GGA TGA GTC CTC TTT G-3' (*Bmal1*); 5'-GAA GAG CTC GGC TTT GAT ACA G-3' and 5'-CAA GGG ATC TGA ACA CAG ATG G-3' (*Cry1*); 5'-CTC AAA AAA CTT ACC AGG GC-3' and 5'-CAC CAC GCT GTG GCG AAA AGT CTG-3' (*p53*); 5'-AGT GCA TTG ACC CTC AGT GGT CTT TCC CCT A-3' and 5'-CAG CTC GTT CCT CCT CTG ACG TTC CAA GAC GTT-3' (*c-Myc*).

One-step RT-PCR was performed with a Light Cycler instrument (Roche Diagnostics, Meylan, France) in a total volume of 20 μL containing 500 ng of total RNA, 7 mM MgCl_2 , 0.75 μM each primer, Light Cycler RT-PCR Reaction Mix SYBR Green I, and Light Cycler RT-PCR Enzyme Mix. All reagents were purchased from Roche. The protocol consisted of four stages: reverse transcription of template RNA, denaturation of the cDNA–RNA hybrid, amplification of cDNA, and melting curve analysis for product identification. Reverse transcription was performed at 55°C for 10 minutes. The denaturation and amplification conditions were 95°C for 30 seconds followed by 40 cycles of PCR. Each cycle of PCR included immediate denaturation at 95°C , 10 seconds of primer annealing at 60°C (59°C for *c-Myc*), and 13 seconds of extension/synthesis at 72°C . At the end of the extension step, the fluorescence of each sample was measured at 84°C (85°C for *Bmal1*) to eliminate the background fluorescence generated by primer dimers. After 40 cycles of amplification, a cDNA melting curve was obtained by heating the samples at $20^{\circ}\text{C}/\text{s}$ to 95°C , cooling them at $20^{\circ}\text{C}/\text{s}$ to 65°C ,

and slowly heating them again at $0.1^{\circ}\text{C}/\text{s}$ to 95°C , whereas fluorescence data were collected at 0.1°C intervals. The intraassay and interassay variation coefficients were less than 1% and less than 6%, respectively. The efficiency of each primer pair to amplify was validated by construction of serial dilution curves and was comparable among all the genes studied, being approximately 90% (data not shown). The specificity of the PCR products was assessed by melting curve analysis and by agarose gel electrophoresis to check for the presence of nonspecific products and to confirm that the size of the product corresponded to that of the expected amplicon.

PCR Data Analysis

The relative levels of each mRNA of the genes of interest were normalized to that of 36B4 by the following formula: relative mRNA level = $2^{(C_p[\text{target gene}] - C_p[\text{reference gene}])}$, where C_p (crossing point) is the cycle number at which the fluorescence signal reaches the threshold of detection. The crossing point was determined using Lightcycler software version 3.5 either using the second derivative maximum method (experiment 1) or using the fit points method (experiment 2). In the fit points method, the noise band was set above the background fluorescence in each run, and the threshold for analysis was adjusted according to the fluorescence level of the known positive standard sample added to each run and related to a previously constructed standard curve using 10-fold serial dilutions. As a result, all six time points were analyzed in duplicate for each gene and each group in a single run. The fit points method was considered as being possibly more precise than the second derivative maximum method and was used in experiment 2 because of the limited number of samples per time point.

Statistical Analysis

Seven-day time series of body temperature ($^{\circ}\text{C}$) and activity data (arbitrary units) of each mouse were analyzed by spectral analysis (Fourier transform analysis) using Mathcad 6.0 (Integral Software, Paris, France), complemented with cosinor analysis for periods of 24, 12, or 8 hours (10,30,31) (data not shown).

For each gene, mean expression was calculated as a function of sampling time, tissue, and experimental condition. Intergroup differences were compared using two-way analysis of variance (ANOVA) for experiment 1. Three-way ANOVA was performed on gene expression data to estimate the respective roles of sampling time, tissue (liver versus tumor), and experimental condition (standard conditions versus chronic jet lag versus combined chronic jet lag and meal timing) and to identify possible interactions in experiment 2.

The statistical significance of sinusoidal rhythmicity was further documented by cosinor analysis (30,31), which characterizes a rhythm by parameters of the fitted cosine function best approximating all data. Periods $\tau = 24$ hours and $\tau = 12$ hours were considered a priori. The rhythm characteristics estimated by this linear least squares method include the mesor (rhythm-adjusted mean), the double amplitude (difference between minimum and maximum of fitted cosine function), and the acrophase (time of maximum in fitted cosine function, with light onset as phase reference). Time measurements are indicated as hours^{minutes}. A rhythm was detected if the null hypothesis was rejected with $P < .05$.

All statistical tests were two-sided. All standard statistical tests were performed using SPSS version 11.5 for Windows software (SPSS, Chicago, IL).

RESULTS

Effects of Chronic Jet Lag on Gene Expression Patterns in Liver of Healthy Mice

Marked 24-hour variations were found for the mRNA expression of the clock genes *Cry1*, *Rev-erba*, *Per2*, and *Bmal1* in the liver of mice synchronized to standard lighting conditions (12 hours of light and 12 hours of darkness for 2–3 weeks) (Fig. 1, left panel). The relative peak-to-trough differences were 10-, 206-, four-, and 26-fold, respectively. All 24-hour changes were statistically validated with both ANOVA and cosinor. Cosinor analysis further documented sinusoidal circadian rhythms for the expression of all four genes, with acrophases occurring in the early light span for *Cry1* and *Rev-erba*, shortly after the light–dark transition for *Per2*, and near the end of the dark span for *Bmal1* (Table 1).

The circadian expression patterns of all four clock genes of mice exposed to conditions mimicking chronic jet lag (10 days of serial 8-hour advances of light–dark cycles every 2 days) were markedly altered compared with those in synchronized mice (Fig. 1, right panel versus left panel). The mean mRNA expression levels of *Cry1*, *Per2*, and *Bmal1* were nearly halved, and that of mean *Rev-erba* expression was more than threefold lower than that of synchronized mice. The *Cry1* and the *Rev-erba* rhythms were severely flattened. The *Per2* rhythm persisted, yet it was dampened, and its peak was shifted back 8 hours (from CT12 to CT4). The *Bmal1* pattern became bimodal, with peaks at CT0 and at CT12. Cosinor analysis indicated that the *Cry1* rhythm was ablated ($P = .23$), yet the minor changes in *Rev-erba* expression over the 24-hour period were fitted with a 12-hour periodic component ($P = .03$) (Table 1). *Per2* expression displayed circadian rhythm despite chronic jet lag, yet with markedly altered characteristics: the mesor was reduced by 40% (0.081 [95% CI = 0.05 to 0.12] compared with 0.13 [95% CI = 0.09 to 0.18] in synchronized mice), and its acrophase advanced by nearly 10 hours (3^{50} [95% CI = 0^{10} to 7^{20}] compared with 14^{20} [95% CI = 10^{20} to 18^{20}] in synchronized mice) (Table 1). Finally, the *Bmal1* rhythm also displayed a statistically significant dominant 12-hour periodic component ($P < .001$) (Table 1).

In synchronized mice, the expression pattern of *c-Myc* was highest at CT8 with low values from CT16 to CT0, whereas *p53* peaked at CT4, with low values from CT8 to CT20 (Fig. 1, left panel). The 24-hour changes were close to statistical significance for the expression of *c-Myc* but not for that of *p53* (P from ANOVA = .055 and .13, respectively); no sinusoidal circadian or 12-hour rhythm was observed with cosinor analysis for either gene (Table 1).

In mice that experienced chronic jet lag, the 24-hour mean expression of *p53* was approximately half that of synchronized mice. *c-Myc* expression increased by nearly 50%, and its rhythmicity was amplified 12-fold over the 24-hour period compared with that in synchronized mice (Fig. 1). Indeed, *c-Myc* expression in the jet-lagged mice followed a sinusoidal circadian rhythm (cosinor $P = .03$), the double amplitude was 235% of the mesor, and acrophase was located near midlight (Table 1).

Based upon two-way ANOVA of the gene expression data, statistically significant differences were found as a function of

circadian time for *Cry1* (two-sided $P = .046$), *Rev-erba* ($P = .001$), and *Bmal1* ($P < .001$), but not *c-Myc* ($P = .055$). The analysis validated differences in mean level of expression between synchronized mice and mice undergoing chronic jet lag for *Rev-erba* ($P = .026$), *Per2* ($P = .035$), *Bmal1* ($P = .01$), and *p53* ($P = .002$). Furthermore, a statistically significant interaction was found between circadian time and light–dark schedule for *Rev-erba* ($P = .002$), *Per2* ($P = .008$), and *Bmal1* ($P < .001$), but not for *c-Myc* ($P = .12$).

Effects of Chronic Jet Lag and Meal Timing in Tumor-Bearing Mice

Meal timing was used here as a means to entrain the circadian clocks otherwise disrupted by chronic jet lag. Meal-fed mice were fed from CT12, the onset of activity, to CT24, the onset of rest.

The body weight of the ad libitum–fed synchronized mice or those that underwent chronic jet lag conditions increased similarly. The meal-fed mice lost weight during the initial 4 days of meal timing, and then their weight increased. The ad libitum–fed mice gained weight slowly during this time. On the day of tumor inoculation, mean body weight (\pm SD) in both groups of the ad libitum–fed mice was 27.7 (± 0.3), and that of the meal-fed mice that had undergone chronic jet lag was 27.1 (± 0.5) (P from ANOVA = .46).

Tumors grew more quickly in the mice undergoing chronic jet lag than in synchronized mice (Fig. 2), whereas restricted feeding moderately counterbalanced the effect of jet lag; the comparison of all three curves with ANOVA indicated statistically significant differences ($P = .04$). On day 12, prior to tissue sampling, mean tumor weight (95% confidence interval [CI]) was 1317 mg (95% CI = 1067 to 1567) in synchronized mice ($n = 13$), 1997 mg (95% CI = 1458 to 2536) in chronic jet-lagged mice fed ad libitum ($n = 14$), and 1567 mg (95% CI = 1032 to 2101) in chronic jet-lagged, meal-fed mice ($n = 15$).

Regardless of light–dark synchronization and meal timing, *Rev-erba*, *Per2*, *Bmal1*, and *c-Myc* mRNA expression in tumor-bearing mice varied over the 24-hour period in liver and in tumor, as indicated by a statistically significant effect of sampling time with three-way ANOVA for each of the genes ($P < .001$, $P = .005$, $P = .048$, and $P = .009$, respectively). By contrast, no temporal change in *p53* expression was statistically validated ($P = .96$). The 24-hour patterns of *Rev-erba* and *Bmal1* expression in liver and tumor differed statistically significantly as a function of light–dark and feeding schedules (*Rev-erba* $P = .002$, *Bmal1* $P = .008$), as indicated by analyzing sampling time by tissue interaction terms with three-way ANOVA. This analysis also showed that the 24-hour patterns of *Per2* and *Bmal1* expression were statistically significantly altered in mice that underwent chronic jet lag or the combination of chronic jet lag and meal timing (*Per2* $P = .019$ and *Bmal1* $P = .001$).

In the livers of tumor-bearing synchronized mice, mRNA levels of *Rev-erba*, *Per2*, and *Bmal1* peaked during the light span; peak-to-trough differences were 36-, 35-, and 32-fold, respectively (Fig. 3, left panel). Sinusoidal 24-hour rhythms in *Rev-erba* and *Per2* mRNA expression were further validated by cosinor analysis (Table 2). For comparison, the respective peak-to-trough differences in *Rev-erba*, *Per2*, and *Bmal1* gene expression were 9.4-, 5.5-, and sixfold in tumor (Fig. 3, right panel);

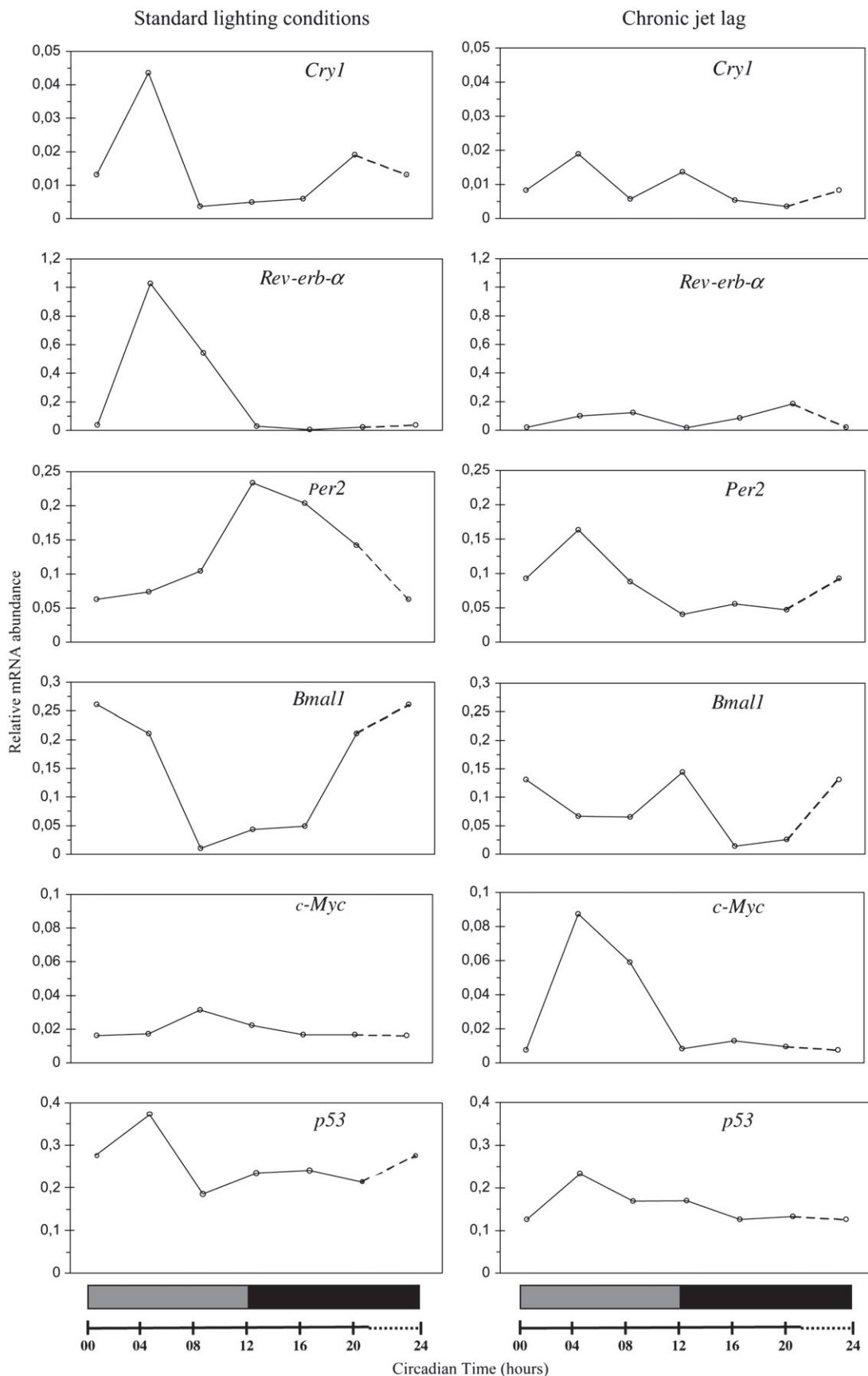


Fig. 1. Circadian expression of clock genes *Cry1*, *Rev-erb α* , *Per2*, *Bmal1*, *c-Myc*, and *p53* in the livers of healthy mice synchronized by standard lighting conditions (**left panel**) or undergoing chronic jet lag (**right panel**). The relative mRNA expression of each gene of interest was normalized to that of *36B4*. Each point represents the mean of 10 mice. The mice in both groups were exposed to

constant darkness during the 2 days preceding sampling. The sampling circadian times (CTs) are relative to the time of light onset, CT0. **Hatched rectangles** indicate subjective light span and **black rectangles** indicate dark span. To better visualize the rhythm during the 24-hour period, data obtained at CT24 and connected with a broken line to data at CT20.

Table 1. Circadian rhythms of gene expression in the liver of healthy, synchronized mice or those undergoing chronic jet lag*

Group	Gene	τ (h)	<i>P</i>	Mesor (95% CI) relative expression	Double amplitude (95% CI), % of mesor	Acrophase (95% CI), hour ^{min}
Synchronized	Cry1	24	.019	0.0217 (0.01 to 0.0323)	203 (27 to 369)	4 ¹⁰ (0 ¹⁰ to 8 ¹⁰)
	Rev-erba	24	.0016	0.2774 (0.1092 to 0.4456)	326 (108 to 541)	5 ²⁰ (2 ³⁰ to 8 ⁰⁰)
	Per2	24	.018	0.1338 (0.0912 to 0.1764)	131 (18 to 239)	14 ²⁰ (10 ²⁰ to 18 ²⁰)
	Bmal1	24	<.001	0.1309 (0.0919 to 0.1699)	204 (92 to 306)	23 ⁴⁰ (21 ⁴⁰ to 25 ⁵⁰)
	c-Myc	24	.39	0.0200 (0.0136 to 0.0264)	62	9 ⁰⁰
	p53	24	.43	0.2532 (0.1992 to 0.3072)	40	2 ³⁰
Chronic jet lag	Cry1	24	.23	0.0092 (0.0036 to 0.0056)	1	5 ⁵⁰
	Rev-erba	24	.82	0.0881 (0.0453 to 0.1309)	43	20 ⁵⁰
		12	.031	0.0881 (0.0476 to 0.1286)	176 (15 to 340)	6 ⁵⁵ (4 ⁴⁰ to 9 ¹⁰) and 18 ⁵⁵ (16 ⁴⁰ to 21 ¹⁰)
	Per2	24	.012	0.0812 (0.0460 to 0.1164)	127 (22 to 222)	3 ⁵⁰ (0 ¹⁰ to 7 ²⁰)
	Bmal1	24	.16	0.0744 (0.0550 to 0.0938)	72	6 ²⁰
		12	<.001	0.0744 (0.0663 to 0.0825)	170 (92 to 247)	11 ⁵⁵ (11 ⁰⁰ to 12 ⁵⁰) and 23 ⁵⁵ (23 ⁰⁰ to 00 ⁵⁰)
	c-Myc	24	.032	0.0307 (0.0119 to 0.0495)	235 (13 to 456)	5 ⁴⁰ (1 ⁰⁰ to 10 ¹⁰)
	p53	24	.09	0.1594 (0.1332 to 0.1856)	52	6 ²⁰

*The relative mRNA level of each gene of interest was normalized to that of 36B4. All circadian parameters are given as means and 95% confidence intervals (CI) using cosinor analysis; *P* values are two-sided. Mesor = rhythm-adjusted mean. Double amplitude = difference between minimum and maximum of the fitted cosine function. Acrophase = time of maximum in fitted cosine function, with light onset as phase reference. A rhythm was detected if the null hypothesis was rejected with *P* < .05.

only Per2 exhibited a sinusoidal circadian rhythm (Table 2). Small variations were found in c-Myc and p53 expression over the 24-hour time period in liver and in tumor, and no sinusoidal waveform was detected (Fig. 3, Table 2).

Mice that underwent chronic jet lag had dampened 24-hour changes in liver and in tumor Rev-erba expression, and the sinusoidal waveform was suppressed, as shown by the lack of any 24-hour rhythm with cosinor (Table 2). Chronic jet lag also clearly altered the circadian patterns in Per2 and Bmal1 mRNA expression in both tissues. In the livers of jet-lagged, tumor-bearing mice, the 24-hour rhythms of Per2 and Bmal1 expression displayed peaks nearly 12 hours out of phase with those in synchronized mice (Fig. 4). Chronic jet lag further ablated the rhythmic changes in tumor Bmal1 expression (Fig. 4, Table 2).

Meal timing restored near-normal rhythmic sinusoidal 24-hour patterns of both Rev-erba and Per2 expression but ablated that of Bmal1 in liver of tumor-bearing mice (Fig. 4, left panel and Table 2). However, meal timing imposed large 24-hour

sinusoidal rhythms in the expression of all three clock genes in tumor tissue (Fig. 4, right panel and Table 2). Chronic jet lag increased the magnitude of the 24-hour changes in p53 and c-Myc expression in both the liver and tumor of the tumor-bearing mice, although a sinusoidal rhythm was seen for p53 in liver only (Fig. 4, Table 2). Meal timing reinforced the c-Myc 24-hour pattern in liver but dampened it in tumor (Fig. 4).

DISCUSSION

Our results demonstrate that chronic jet lag severely altered the circadian rhythms in the expression of clock genes in liver and tumor of mice bearing Glasgow osteosarcoma tumors. We also observed modifications in the expression patterns of the downstream genes c-Myc and p53 and accelerated tumor growth compared with that in control synchronized mice. Meal timing (i.e., from CT12, the onset of activity, to CT24, the onset of rest) prevented the alterations produced by chronic jet lag in the expression patterns of Per2 and Rev-erba in liver and tumor and Bmal1 in tumor and slowed tumor growth.

We previously reported (11) that an 8-hour advance of light onset every 2 days markedly alters the circadian patterns of rest-activity and body temperature, two main circadian outputs that are directly controlled by the suprachiasmatic nuclei, the central pacemaker in the hypothalamus. In this study, similar results were obtained in both healthy mice and mice bearing tumors (data not shown).

The transcription of clock genes Cry1, Rev-erba, Per2, and Bmal1 varied largely as a function of circadian time in the liver of synchronized healthy mice, with peak times and amplitudes similar to those in previous reports (1,3,6,12,32). Over a 24-hour period, the mean maximum expression of Cry1 was nearly sixfold lower than mean maximum expression of Per2 or Bmal1 and 25-fold lower than that of Rev-erba. For this reason, only the last three clock genes were measured in mice with Glasgow osteosarcoma. For Rev-erba, Per2, and Bmal1, mRNA expression in the liver of tumor-bearing mice displayed circadian changes that were similar to those of healthy mice. The 24-hour patterns in mean Rev-erba or Per2 expression as determined here with quantitative RT-PCR were in agreement with those previously reported using

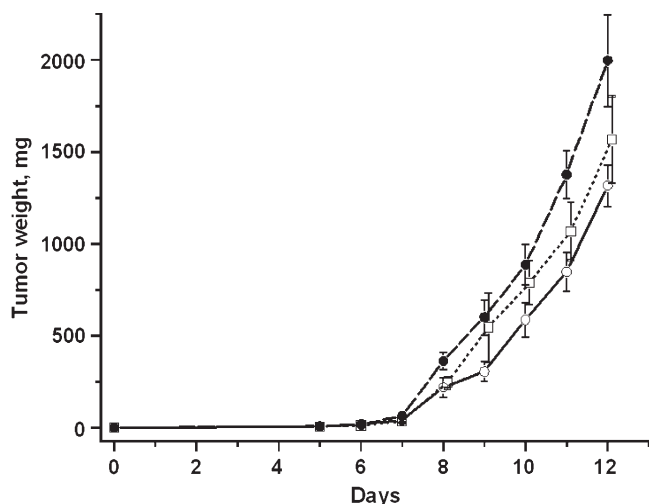


Fig. 2. Tumor growth in mice synchronized by standard lighting conditions (dashed line, *n* = 13), undergoing chronic jet lag (solid line, *n* = 14), or the combination of meal timing and chronic jet lag (dotted line, *n* = 15). Mean tumor weight and 95% confidence intervals at each time point over the 12-day span following inoculation of Glasgow osteosarcoma are shown.

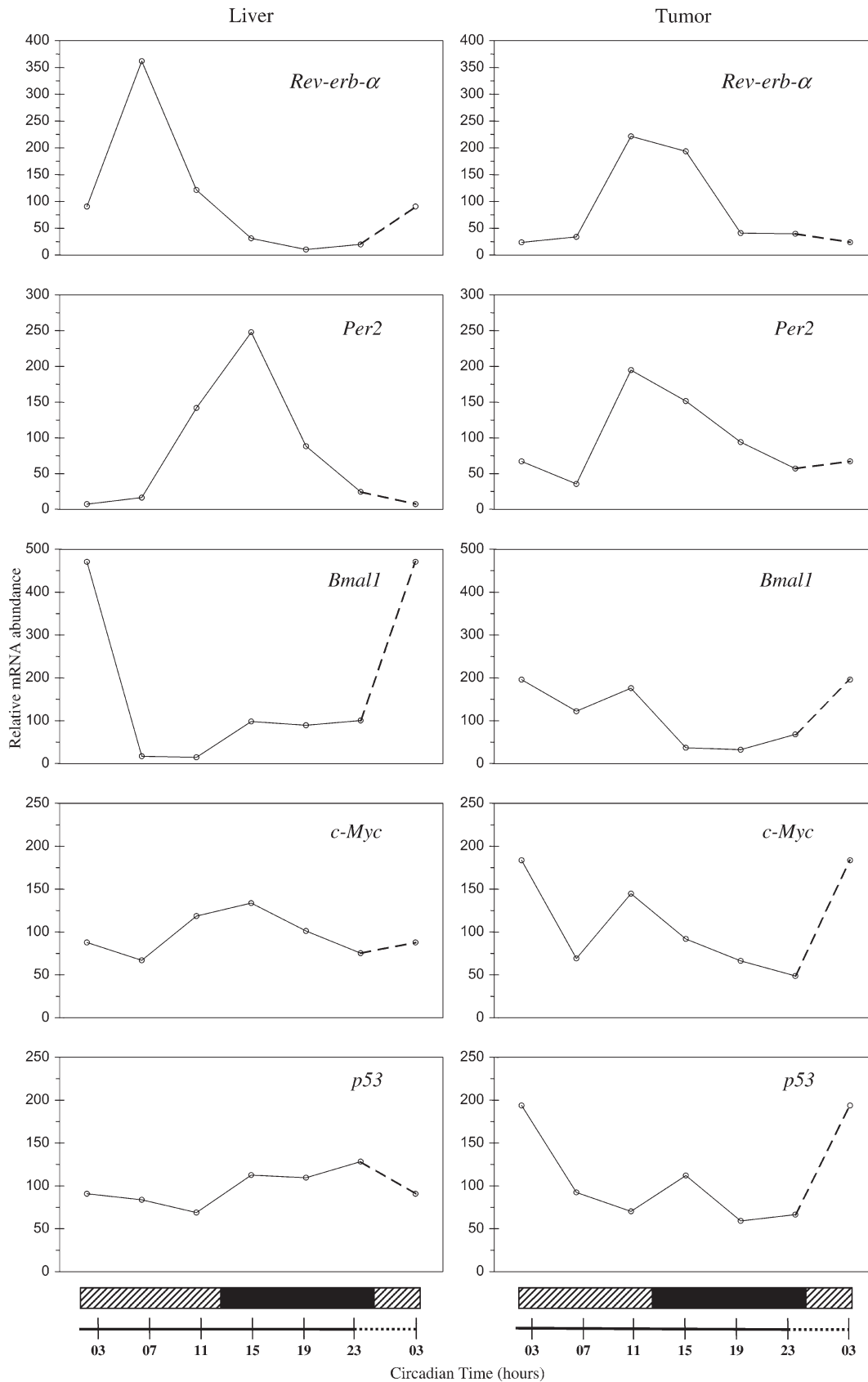


Fig. 3. Circadian expression of clock genes *Rev-erb α* , *Per2*, *Bmal1*, *c-Myc*, and *p53* in the livers (**left panel**) or the tumors (**right panel**) of tumor-bearing mice synchronized to standard lighting conditions. The relative mRNA expression of each gene of interest was normalized to that of 36B4. Gene expression was calculated as a percentage of the 24-hour mean value in each group. Each point represents the mean of two to three mice. The mice in both groups

were exposed to constant darkness during the 2 days preceding sampling. The sampling circadian times (CTs) are relative to the time of light onset, CT0. To better visualize the rhythm during the 24-hour period, data obtained for CT3 are repeated 24 hours later and connected with a broken line to data at CT23. **Hatched rectangles** indicate subjective light span and **black rectangles** indicate dark span.

Table 2. Circadian rhythms of gene expression in tumor-bearing mice synchronized, undergoing chronic jet lag, or undergoing chronic jet lag and meal timing*

Group	Tissue	Gene	P	Double amplitude (95% CI), % of mesor	Acrophase (95% CI), hour ^{min}
Synchronized	Liver	Rev-erb α	.009	290 (78 to 503)	7 ²⁰ (4 ⁴⁰ to 10 ⁰⁰)
		Per2	.006	238 (196 to 280)	14 ⁴⁰ (11 ⁴⁰ to 17 ⁴⁰)
		Bmal1	.38	166	00 ⁵⁰
		c-Myc	.42	59	14 ⁴⁰
		p53	.33	50	20 ³⁰
	Tumor	Rev-erb α	.18	206	13 ⁰⁰
		Per2	.03	130 (119 to 249)	13 ⁴⁰ (9 ²⁰ to 18 ⁰⁰)
		Bmal1	.05	155	6 ¹⁰
		c-Myc	.55	64	7 ¹⁰
		p53	.73	57	4 ³⁰
Chronic jet lag	Liver	Rev-erb α	.54	77	4 ²⁰
		Per2	.049	138 (1 to 277)	6 ⁴⁰ (0 ⁴⁰ to 12 ⁴⁰)
		Bmal1	.027	192 (22 to 362)	15 ⁰⁰ (11 ⁰⁰ to 19 ⁰⁰)
		c-Myc	.32	87.6	9 ⁰⁰
		p53	.003	171 (66 to 275)	17 ⁰⁰ (14 ³⁰ to 19 ³⁰)
	Tumor	Rev-erb α	.17	118	9 ¹⁰
		Per2	.90	25	14 ⁴⁰
		Bmal1	.55	54	2 ⁵⁰
		c-Myc	.36	161	7 ¹⁰
		p53	.41	77	4 ⁴⁰
Chronic jet lag + meal timing	Liver	Rev-erb α	.008	263 (70 to 456)	7 ⁰⁰ (3 ⁵⁰ to 10 ¹⁰)
		Per2	.009	188 (48 to 329)	13 ³⁰ (10 ²⁰ to 16 ⁴⁰)
		Bmal1	.88	22	2 ²⁰
		c-Myc	.03	182 (16 to 348)	6 ⁵⁰ (2 ³⁰ to 11 ¹⁰)
		p53	.72	41	12 ¹⁰
	Tumor	Rev-erb α	.07	127	7 ¹⁰
		Per2	.01	223 (40 to 406)	6 ⁵⁰ (3 ³⁰ to 10 ¹⁰)
		Bmal1	.01	140 (28 to 251)	4 ⁴⁰ (1 ⁰⁰ to 8 ²⁰)
		c-Myc	.35	93	7 ⁰⁰
		p53	.77	76	11 ⁵⁰

*The relative mRNA level of each gene of interest was normalized to that of 36B4. Due to the method used, all mesors were ~100%. All circadian parameters are given as means and 95% confidence intervals (CI). Mesor = rhythm-adjusted mean. Double amplitude = difference between minimum and maximum of the fitted cosine function. Acrophase = time of maximum in fitted cosine function, with light onset as phase reference. A rhythm was detected if the null hypothesis was rejected with $P < .05$.

RNase protection assay and only four time-points (11). However, this study showed that, in tumor-bearing mice, the waveform of Bmal1 mRNA expression in liver was modified so that the sinusoidal rhythm observed in healthy mice was not detected. Nevertheless, the overall characteristics of the liver molecular clock were only slightly affected by the presence of a tumor since the transcriptional activity of the positive feedback loop of the clock, here assessed with Rev-erb α and Bmal1 (32), peaked in the first half of the light span, and the transcriptional activity of the negative feedback loop peaked near the transition from light to darkness, as is the case in healthy mice.

Chronic jet lag markedly reduced the average level of clock gene expression and severely altered their rhythms in healthy mouse liver. Interindividual variability in clock gene expression was reduced in the mice that underwent chronic jet lag compared with synchronized mice, suggesting that the ablation of circadian rhythmicity could not result from increased interindividual variability in circadian phases. Instead, it is likely that the rhythms were indeed ablated in each mouse.

Chronic jet lag further revealed differences in the molecular clock response to environmental changes between healthy mice and tumor-bearing ones. Chronic jet lag induced bimodality in the Rev-erb α and Bmal1 expression patterns of the liver clock in healthy mice. In tumor-bearing mice, by contrast, chronic jet lag suppressed the circadian rhythm in Rev-erb α , a result similar to that of a previous report using RNase protection assay (11). Chronic jet lag also shifted the Bmal1 circadian rhythm back by

nearly 14 hours compared with that of synchronized mice. The relationship between Per2 and Bmal1 peak expression over the circadian time scale constitutes the core part of a functional molecular clock (33). Chronic jet lag altered this relationship in the liver of healthy mice but maintained it in the liver of tumor-bearing mice, although with an advance of nearly 8 hours. Thus, the tumor itself could have a role in the entrainment of the liver clock, in the absence of fit host circadian coordination.

Meal timing entrains circadian rhythms in the expression of clock genes and clock-controlled genes in liver and in other peripheral oscillators (23,24), even in the absence of the hypothalamic pacemaker (27). We found that meal timing prevented the circadian patterns of Rev-erb α and Per2 mRNA expression from being disrupted by chronic jet lag, yet Bmal1 rhythm was suppressed. This finding suggests that only some molecular components of the liver circadian clock can be entrained by meal timing.

The effects of light and food schedule on gene expression were further investigated in the tumor. Tumor Per2 and Bmal1 transcription remained rhythmic in light-dark synchronized mice. The time lag between expression peaks in tumor differed from that in liver, however, and the pattern of Rev-erb α expression in tumor, was dampened compared with that in liver. This finding suggested that the tumor clock was altered despite photoperiodic synchronization. The observation that chronic jet lag clearly ablated sinusoidal circadian rhythms in clock gene expression in the tumor raises the possibility that additional molecular clock

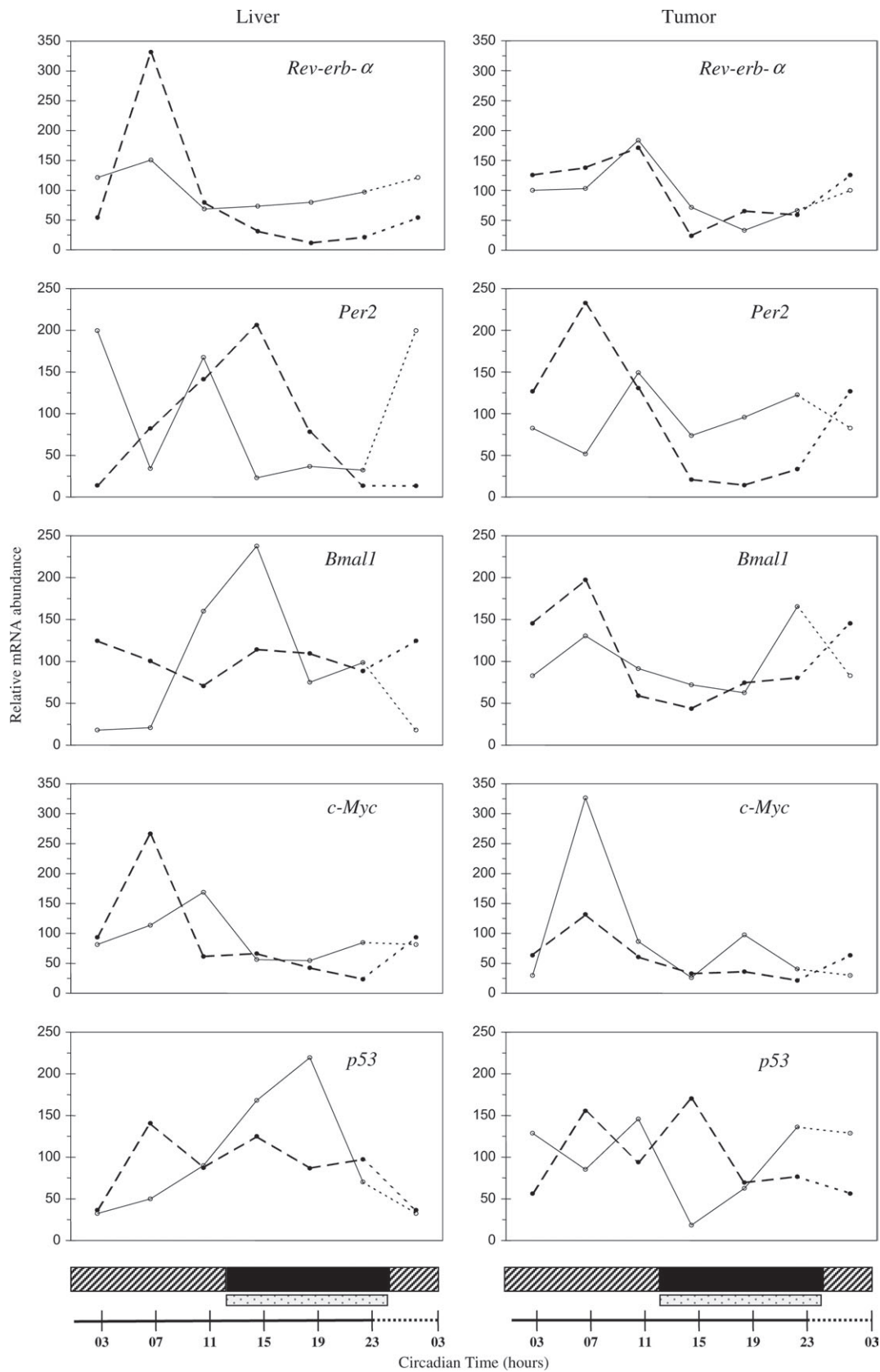


Fig. 4. Data for 24-hour changes in the mRNA expression of *Rev-erb-α*, *Per2*, *Bmal1*, *c-Myc*, and *p53* in the livers (left panel) or the tumors (right panel) of tumor-bearing mice undergoing chronic jet lag (solid line) or the combination of meal timing and chronic jet lag (dashed line). The relative mRNA expression of each gene of interest was normalized to that of *36B4*. Gene expression was calculated as a percentage of the 24-hour mean value in each group. Each point

represents the mean of two to three mice. The mice in both groups were exposed to constant darkness during the 2 days preceding sampling. The sampling circadian times (CT) are relative to subjective time of light onset, CT0. To better visualize the rhythm during the 24-hour period, data obtained at CT3 are repeated 24 hours later and connected with a broken line to data at CT23. **Hatched rectangles** indicate subjective light span and **black rectangles** indicate dark span.

deregulation within the tumor itself leads to subsequent tumor progression, in agreement with prior observations (10,11). By contrast, the combination of meal timing and chronic jet lag induced nearly synchronous rhythmic 24-hour changes in *Rev-erb α* , *Bmal1*, and *Per2* expression in the tumor. Because ad libitum- and meal-fed mice had similar weights when tumors were injected, we believe that the tumor growth differences in these two groups were not related to food restriction but rather depended upon the expression patterns of the molecular clock and cell cycle genes. The restored tumor molecular clock exerted a modest yet effective negative control of tumor progression, despite the atypical phase relations within the clock's core mechanisms. In agreement with this, the restriction of food availability to 4–6 hours during the light span was able to largely slow the growth of Glasgow osteosarcoma (25). Thus, selective inhibition of certain components of the tumor molecular clock would speed up malignant growth through accelerated cell cycle progression, stimulated angiogenesis, or reduced apoptosis, whereas partial restoration or reinforcement of the tumor molecular clock would slow down malignant growth through opposite effects on these mechanisms.

Cell cycle phase distribution and apoptotic pathways are under circadian regulation in healthy, rapidly proliferating tissues, such as bone marrow (16,34–36). In tumors, G₂/M gating and tumor angiogenesis are well coordinated by the circadian system, whereas the G₁/S transition or apoptotic pathways display temporal changes in different tumor types (17,21,37,38). In the liver of healthy mice, we found that the severe clock dysfunction produced by chronic jet lag increased the overall level of c-Myc expression and amplified its rhythm and nearly halved the overall level of p53 expression. Our results, obtained with functional clock disruption, parallel those reported in mice with germinal *Per2* null mutation (12). *Per2*^{-/-} mice displayed disrupted circadian clock function and displayed an increased susceptibility to develop cancers following exposure to γ -radiation (12). Thus, chronic jet lag exposure could also favor carcinogenesis through increased cellular proliferation and subsequent genomic instability induced by carcinogenic exposure. Indeed, a single 8-hour advance in the light–dark cycle also decreased apoptosis in the mammary tissues of mice exposed to γ -radiation (39). Both promotion and progression of liver tumors resulted from prolonged exposure of rats to constant light (7,40), a lighting condition that disrupts the circadian system of rats (41). In another rat model, accelerated tumor progression was related to enhanced tumor fatty acid uptake and metabolism, supporting a role for food intake in malignant progression (40).

In tumor-bearing mice, the molecular clock of the tumor clearly interacted in a complex manner with the host's response to chronic jet lag and to the combination of chronic jet lag and meal timing, as indicated by observed changes in liver c-Myc and p53 transcriptional activities under these conditions. Interestingly, the combination of meal timing and chronic jet lag dampened the 24-hour variations in c-Myc and p53 expression in the tumor, suggesting that negative regulation of proliferation was stronger in the “restored” yet altered tumor circadian clock.

The results from this study do not rule out the possibility that light and food schedules modify transcriptional activity of only a few genes in the molecular clock and the cell cycle without further downstream consequences. This possibility is unlikely because light and food schedules have been repeatedly shown to alter tumor progression (10,25). In addition, potential downstream

consequences of altered transcription of clock genes and cell cycle genes other than tumor growth suppression were not investigated in this study. Indeed, light and food schedules could also modify the dynamic patterns in transcription of other clock and cell cycle genes and may also affect translation, conformation, and/or heterodimerization of clock and cell cycle proteins. Systematic exploration of the crosstalk between the circadian clock and the cell cycle in cancer processes will be necessary to provide new therapeutic opportunities to prevent or treat cancers.

Several epidemiologic studies emphasize the clinical relevance of our findings because people in repeatedly altered environmental cycles through prolonged shift work or iterative transmeridian flights had a statistically significantly increased risk of breast or colorectal cancer compared with that of people who are exposed to regular 24-hour cycles (42–47).

In conclusion, we showed here that the molecular clocks in liver and in tumor were severely altered by the disruption of regular photoperiodic synchronization, a condition that also accelerated tumor growth. The deleterious effects of jet lag on the molecular clock in liver tissue were partly counteracted by meal timing, and more so in the tumor itself, the growth of which was slowed. The effects were partly mediated by the relationship between the molecular clock and the expression patterns of c-Myc and p53.

REFERENCES

- (1) Hastings MH, Reddy AB, Maywood ES. A clockwork web: circadian timing in brain and periphery, in health and disease. *Nat Rev Neurosci* 2003;4:649–61.
- (2) Klein DC, Moore RY, Reppert SM. *Suprachiasmatic nucleus, the mind's clock*. Oxford University Press, Oxford; 1991.
- (3) Reppert SM, Weaver DR. Coordination of circadian timing in mammals. *Nature* 2002;418:935–41.
- (4) Le Minh N, Damiola F, Tronche F, Schutz G, Schibler U. Glucocorticoids inhibit food-induced phase-shifting in peripheral circadian oscillators. *EMBO J*. 2001;20:7128–36.
- (5) Matsuo T, Yamaguchi S, Mitsui S, Emi A, Shimoda F, Okamura H. Control mechanism of the circadian clock for timing of cell division in vivo. *Science* 2003;302:255–59.
- (6) Schibler U, Sassone-Corsi P. A web of circadian pacemakers. *Cell* 2002;111:919–22.
- (7) Shah PN, Mhatre ML, Kothari L. Effect of melatonin on mammary carcinogenesis in intact and pinealectomized rats in varying photoperiods. *Cancer Res* 1984;44:3403–7.
- (8) van den Heiligenberg S, Depres-Brummer P, Barbason H, Claustrat B, Reynes M, Levi F. Promoting effect of constant light exposure on diethylnitrosamine-induced hepatocarcinogenesis in rats. *Life Sci* 1999;64:2523–34.
- (9) Wille JJ Jr. Circadian rhythm of tumor promotion in the two-stage model of mouse tumorigenesis. *Cancer Lett* 2003;190:143–9.
- (10) Filipinski E, King VM, Li XM, Granda TG, Mormont MC, Liu X, et al. Host circadian clock as a control point in tumor progression. *J Natl Cancer Inst* 2002;94:690–7.
- (11) Filipinski E, Delaunay F, King VM, Wu MW, Claustrat B, Grechez-Cassiau A, et al. Effects of chronic jet lag on malignant growth in mice. *Cancer Res* 2004;64:7879–85.
- (12) Fu L, Pelicano H, Liu J, Huang P, Lee CC. The circadian gene *Period2* plays an important role in tumor suppression and DNA damage response in vivo. *Cell* 2002;111:41–50.
- (13) Nagoshi E, Saini C, Bauer C, Laroche T, Naef F, Schibler U. Circadian gene expression in individual fibroblasts: cell-autonomous and self-sustained oscillators pass time to daughter cells. *Cell* 2004;119:693–705.
- (14) Scheving LE, Burns ER, Pauly JE, Tsai TH. Circadian variation in cell division of the mouse alimentary tract, bone marrow and corneal epithelium. *Anat Rec* 1978;191:479–86.

- (15) Bjarnason GA, Jordan R. Circadian variation in the expression of cell-cycle proteins in human oral epithelium. *Am J Pathol* 1999;154:613–22.
- (16) Smaaland R, Laerum OD, Lote K, Sletvold O, Sothorn RB, Bjerknes R. DNA synthesis in human bone marrow is circadian stage dependent. *Blood* 1991;77:2603–11.
- (17) Granda TG, Levi F. Tumor-based rhythms of anticancer efficacy in experimental models. *Chronobiol Int* 2002;19:21–41.
- (18) Matsumura I, Tanaka H, Kanakura Y. E2F1 and c-Myc in cell growth and death. *Cell Cycle* 2003;2:333–8.
- (19) Hofseth LJ, Hussain SP, Harris CC. p53: 25 years after its discovery. *Trends Pharmacol Sci* 2004;25:177–81.
- (20) Kellog DR. Wee1-dependent mechanisms required for coordination of cell growth and cell division. *J Cell Sci* 2003;116:4883–90.
- (21) Granda TG, Liu XH, Cermakian N, Smaaland R, Filipiński E, Sassone-Corsi P, et al. Circadian regulation of cell cycle and apoptosis proteins in mouse bone marrow and tumor. *FASEB J* 2005;19:304–6.
- (22) Fu L, Lee CC. The circadian clock: pacemaker and tumour suppressor. *Nat Rev Cancer* 2003;3:350–61.
- (23) Damiola F, Le Minh N, Preitner N, Kornmann B, Fleury-Olela F, Schibler U. Restricted feeding uncouples circadian oscillators in peripheral tissues from the central pacemaker in the suprachiasmatic nucleus. *Genes Dev* 2000;14:2950–61.
- (24) Stokkan KA, Yamazaki S, Tei H, Sakaki Y, Menaker M. Entrainment of the circadian clock in the liver by feeding. *Science* 2001;291:490–3.
- (25) Wu MW, Li XM, Xian LJ, Levi F. Effects of meal timing on tumor progression in mice. *Life Sci* 2004;75:1181–93.
- (26) Granda TG, d'Attino RM, Filipiński E, Vrignaud P, Bissery MC, Garufi C, et al. Circadian optimization of irinotecan efficacy in mice with Glasgow osteosarcoma. *Br J Cancer* 2002;86:999–1005.
- (27) Hara R, Wan K, Wakamatsu H, Aida R, Moriya T, Akiyama M, et al. Restricted feeding entrains liver clock without participation of the suprachiasmatic nucleus. *Genes Cells* 2001;6:269–78.
- (28) Marques MD, Waterhouse JM. Masking and the evolution of circadian rhythmicity. *Chronobiol Int* 1994;11:146–55.
- (29) Bryant S, Manning DL. Formaldehyde gel electrophoresis of total RNA. *Methods Mol Biol* 1998;86:69–72.
- (30) Nelson W, Tong YL, Lee JK, Halberg F. Methods for cosinor-rhythmometry. *Chronobiologia* 1979;6:305–23.
- (31) De Prins J, Hecquet B. Data processing in chronobiological studies. In: Touitou Y, Haus E, editors. *Biologic rhythms in clinical and laboratory medicine*. Berlin Heidelberg: Springer; 1992. p. 90–112.
- (32) Preitner N, Damiola F, Lopez-Molina L, Zakany J, Duboule D, Albrecht U, et al. The orphan nuclear receptor REV-ERB α controls circadian transcription within the positive limb of the mammalian circadian oscillator. *Cell* 2002;110:251–60.
- (33) Leloup JC, Goldbeter A. Toward a detailed computational model for the mammalian circadian clock. *Proc Natl Acad Sci U S A* 2003;100:7051–6.
- (34) Laerum OD. Hematopoiesis occurs in rhythms. *Exp Hematol* 1995;23:1145–7.
- (35) Tampellini M, Filipiński E, Liu XH, Li XM, Francois E, Levi F. Circadian rhythm in docetaxel tolerability and efficacy in mice. *Cancer Res* 1998;58:3896–904.
- (36) Filipiński E, King VM, Etienne MC, Li XM, Claustrat B, Granda TG, et al. Persistent twenty-four hour changes in liver and bone marrow despite suprachiasmatic nuclei ablation in mice. *Am J Physiol Regul Integr Comp Physiol* 2004;287:R844–51.
- (37) Koyanagi S, Nakagawa H, Kuramoto Y, Ohdo S, Soeda S, Shimeno H. Optimizing the dosing schedule of TNP-470 (O-(chloroacetyl-carbamoyl) fumagillol) enhances its antitumor and antiangiogenic efficacies. *J Pharmacol Exp Ther* 2003;304:669–74.
- (38) Koyanagi S, Kuramoto Y, Nakagawa H, Aramaki H, Ohdo S, Soeda S, et al. A molecular mechanism regulating circadian expression of vascular endothelial growth factor in tumor cells. *Cancer Res* 2003;63:7277–83.
- (39) Petit LM, Jerry DJ, Bittman EL, Harrington ME. Effects of circadian rhythm disruption on radiation-induced apoptosis. Ninth Meeting of Society for Research on Biological Rhythms; 2004 Jun 24–26; Whistler, BC, Canada, abstract 154.
- (40) Dauchy RT, Blask DE, Sauer L, Brainard GC, Krause JA. Dim light during darkness stimulates tumor progression by enhancing tumor fatty acid uptake and metabolism. *Cancer Lett* 1999;144:131–6.
- (41) Depres-Brummer P, Bourin P, Pages N, Metzger G, Levi F. Persistent T lymphocyte rhythms despite suppressed circadian clock outputs in rats. *Am J Physiol* 1997;273(6 Pt 2):R1891–9.
- (42) Schernhammer ES, Laden F, Speizer FE, Willett WC, Hunter DJ, Kawachi I, et al. Rotating night shifts and risk of breast cancer in women participating in the Nurses' Health Study. *J Natl Cancer Inst* 2001;93:1563–8.
- (43) Schernhammer ES, Laden F, Speizer FE, Willett WC, Hunter DJ, Kawachi I, et al. Night-shift work and risk of colorectal cancer in the nurses' health study. *J Natl Cancer Inst* 2003;95:825–8.
- (44) Davis S, Mirick DK, Stevens RG. Night shift work, light at night, and risk of breast cancer. *J Natl Cancer Inst* 2001;93:1557–62.
- (45) Hansen J. Light at night, shift work, and breast cancer risk. *J Natl Cancer Inst* 2001;93:1513–5.
- (46) Pukkala E, Aspholm R, Auvinen A, Eliasch H, Gundestrup M, Haldorsen T, et al. Incidence of cancer among Nordic airline pilots over five decades: occupational cohort study. *BMJ* 2002;325:567–71.
- (47) Rafnsson V, Tulinius H, Jonasson JG, Hrafnkelsson J. Risk of breast cancer in female flight attendants: a population-based study (Iceland). *Cancer Causes Control* 2001;12:95–101.

NOTES

E. Filipiński, P. F. Innominato, and M. W. Wu contributed equally to this work.

Supported by INSERM Action Thématique Concertée Nutrition (Project A01039LS), Programme de Recherches Avancées de Coopération Franco-Chinoises (PRA B00–07), Association pour la Recherche sur le Temps Biologique et la Chronothérapie and Association pour la Recherche sur le Cancer (grant 3342), Paul Brousse Hospital, Villejuif, France, and Clinical Important Program of Ministry of Public Health of P.R. China (No. 20014056).

Manuscript received August 23, 2004; revised December 22, 2004; accepted February 1, 2005.